

Experimental Evaluation of Oil Film Thicknesses in a Tilting Pad Hydrodynamic Thrust Bearing

Vilmar Arthur Schwarz

Universidade Federal de Itajubá, Instituto de Mecânica, CP 50 , CEP 37500-903, Itajubá, MG, Brasil
vilmar@unifei.edu.br

André Garcia Chiarello

Universidade Federal de Itajubá, Instituto de Mecânica, CP 50 , CEP 37500-903, Itajubá, MG, Brasil
andregc@unifei.edu.br

Marcos Moura Galvão

Universidade Federal de Itajubá, Instituto de Mecânica, CP 50 , CEP 37500-903, Itajubá, MG, Brasil
marcosmgvg@ig.com.br

Abstract. *This work deals with the experimental determination of oil film thicknesses in a tilting pad hydrodynamic thrust bearing. A rotating test machine with vertical rotor has been constructed with a hydrodynamic thrust bearing with sector pads pivoted at 66% of the pad angle. The hydrodynamic bearing was properly adapted to accommodate non-contact type of inductive displacement sensors, conveniently set to achieve oil film thicknesses at several pad positions. A dynamic data acquisition system and the Matlab software have been used to evaluate the geometric displacements of a particular bearing pad under different operational machine conditions. The influences of the rotor angular velocity, the lubricant oil flow rate and the bearing axial load were evaluated and the preliminary experimental results have shown that oil film thickness variation occurs in both circumferential and radial directions.*

Keywords: *oil film thickness, hydrodynamic bearing,, sector pads, friction torque, temperatures.*

1. Introduction

There are few data in the literature about experimentally obtaining the thicknesses of the oil film established between the rotating collar and the bearing pads. The results were usually obtained on horizontal shaft thrust bearings with centrally pivoted or fixed pads, such as Gregory (1974) by measuring oil film thickness and pad under babbitt surface temperatures of a double six tilting pad thrust bearing with 133.55 mm inner diameter and 266.7 mm outer diameter, pad arc length 51° and a total bearing surface area of 35548 mm^2 . An ISO VG32 mineral oil was used, oil film thickness being on the order of $25 \mu\text{m}$ and $45 \mu\text{m}$, respectively, for the loaded and the unloaded side of the double thrust bearing. Speeds varied from 4000 rpm to 11000 rpm and loads (unit pressure) from 0.7 to 2.1 MPa.

Dadouch et al. (2000) obtained experimental data on oil film thickness, pad surface temperatures, and pressure distribution for a vertical shaft thrust bearing consisted of eight fixed pads with 200 mm outer diameter, with loads and speeds up to 8 kN and 2600 rpm respectively. For a rotational speed of 2000 rpm and thrust loads varying from 1 to 8 kN, minimum oil film thicknesses values of $130 \mu\text{m}$ to $45 \mu\text{m}$, respectively, were obtained. However, this range of thrust load seems to be somewhat light, in respect to the bearing size.

Yuan et al. (1999) presented the description of a laboratory test rig for measurement of oil film thickness and distribution of both temperature and pressure on the surfaces of two pads of a 12 spring supported sector pads thrust bearing with inner and outer diameters equal to 711 mm and 1168 mm, respectively. For the highest condition of speed and load, 500 rpm and 4 MPa, respectively, a top temperature of about 100°C at the mean radius and about 88°C near the inner radius of a pad were recorded.

Glavatskikh (2001) presented a wide range of experimental data obtained from a horizontal shaft flooded thrust bearing with six steel-backed babbitt-faced pads pivoted at 60% of the pad angle, the inner and outer diameters being equal to 114.3 mm and 228.6 mm, respectively. An ISO VG46 mineral oil supplied at 30°C , 40°C and 60°C with a constant 15 l/min. flow rate was employed, rotational speed ranging from 1500 rpm to 3000 rpm. Minimum oil film thicknesses varied from $20 \mu\text{m}$ to $60 \mu\text{m}$, while oil film thicknesses near the leading edge of the pad ranged from about $50 \mu\text{m}$ to $145 \mu\text{m}$.

In a more recent paper, Glavatskikh and DeCamillo(2004) presented the corresponding experimental data for the same bearing, but lubricated with an ISO VG32 and an ISO VG68 lubricant oils, instead of the ISO VG46 of the previous paper.

The main objective of the present paper is to carry out an experimental testing on the thicknesses of the oil film established between the rotating collar and the pivoted pads, bearing friction torque and temperature distribution throughout a vertical shaft tilting pad thrust bearing, for a wide range of speed, load and lubrication conditions. This was achieved through a high-speed data acquisition system which logs out the signals from the proximity sensors, torque transducer, thermocouples and load cells.

2. The Test-Rig

The general arrangement of the test rig is shown in Fig.1. Power is supplied by a 5kW variable speed d.c. electric motor, allowing a step less speed variation from 0 to 3500 rpm. Just below the electric motor, a torque transducer HBM T10F allows continuous monitoring of torques from 0 to 100 N.m. Right down, a flexible coupling Antares AT50 is used to connect the main shaft/rotating collar to the torque transducer/electric motor.

The test module proper, i.e., the Kingsbury KV9" thrust bearing, rigidly clamped to the oil reservoir, is lubricated by an ISO VG 32 mineral oil supplied by means of an hydraulic unit with heat exchanger, enabling to control the inlet oil at any required temperature from 40°C to 60°C. Thrust load to the bearing is applied through the hydraulic jack and is measured simultaneously by a load cell inserted in one of the upper leveling plates, as shown in Fig. 3, and by the main load cell, centrally positioned on top of the jack. Reaction to the applied load is provided by the rolling contact bearing housing seen right bellow the flexible coupling.

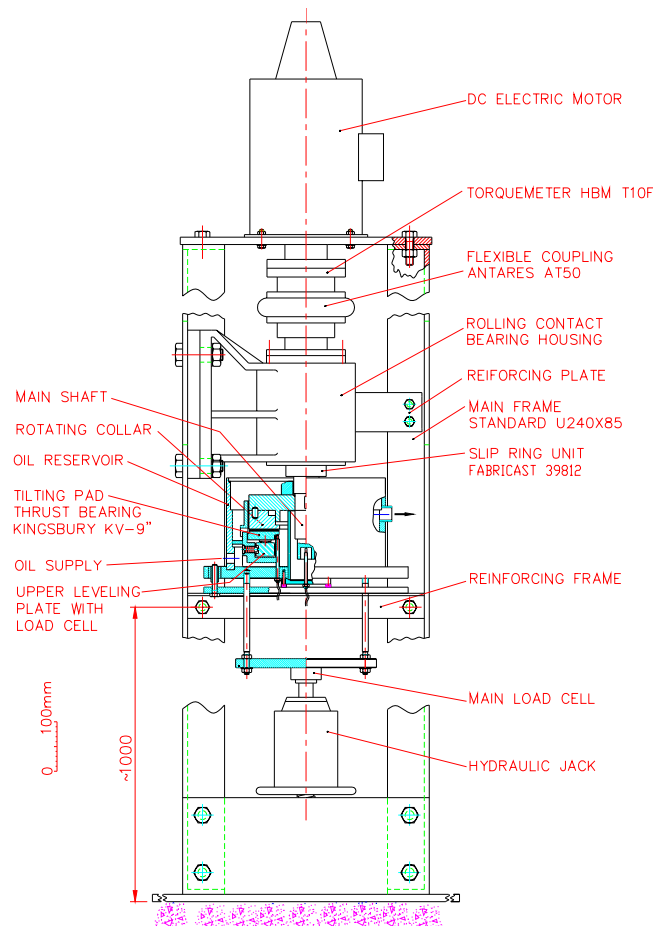


Figure 1. General arrangement of the test-rig

3. The test module

The test module, as shown in Fig.2 consists mainly by the drive spindle (23), rotating collar (20), tilting pads (16), showing the babbitt coating on top and the spherical pivot on the bottom, leveling plates (14), base ring (13) and oil reservoir which is composed by two concentric tubes (17) and (18) and base plate (9). Ring (15) is installed between the base ring (13) and the outer tube of the oil reservoir, in order to drive the supplied oil through six radial channels existing in the bottom of the base ring. In this way, the supplied oil is driven from the outer to the inner radii of the base ring, up to the inner radius of the pads and then it flows radially from the inner to the outer radii of the pads, through the six radial channels existing between them. Rotation of the collar carries the oil over the working surfaces of the pads. An ISO VG32 mineral oil with viscosities of 27.2 mPa.s at 40°C and 4.6 mPa.s at 100°C, was used.

Two non-contact inductive displacement sensors (Bentley Nevada™ Proximity 3300 series) were appropriately fixed to the base plate (9), in order to monitor the axial displacements of one of the bearing pads. Similarly, an identical proximity sensor (5) was conveniently installed to monitor the axial displacement of the shaft (23) together with the

rotating collar (20). The Lynx™ digital signal analyzer was utilized for signal acquisition and processing. Matlab™ software routines were elaborated for calculating the oil film thickness.

Thrust load is applied through a hydraulic jack positioned just below the load cell (01), which measures the load, which is transferred from the load disc (02) to the base plate (09), base ring (13) and the tilting pads through the three vertical rods (03). In this way, the load is applied upwards from the pads against the rotating collar. Bearing friction torque is measured through an HBM T10F torque transducer, which access the total torque from both the tilting pads thrust bearing itself, and two rolling contact bearings that counteracts the applied thrust load. The Temperature measurement is accomplished by using type K (chromel/alumel) thermocouples embedded at several positions within two pads. Also, the temperatures of the oil supplied to the bearing assembly at the inlet and outlet positions in the reservoir are measured through two thermocouples conveniently installed at the inlet and outlet oil lines. For most of the tests, the lubricant oil was supplied at 45°C, although some tests were carried out with inlet oil temperatures from 40°C to 65°C in steps of 5°C. Rotating speed is adjusted by the current converter that controls the d.c. motor and accurately measured by a Minipa MDT2244 optical digital tachometer.

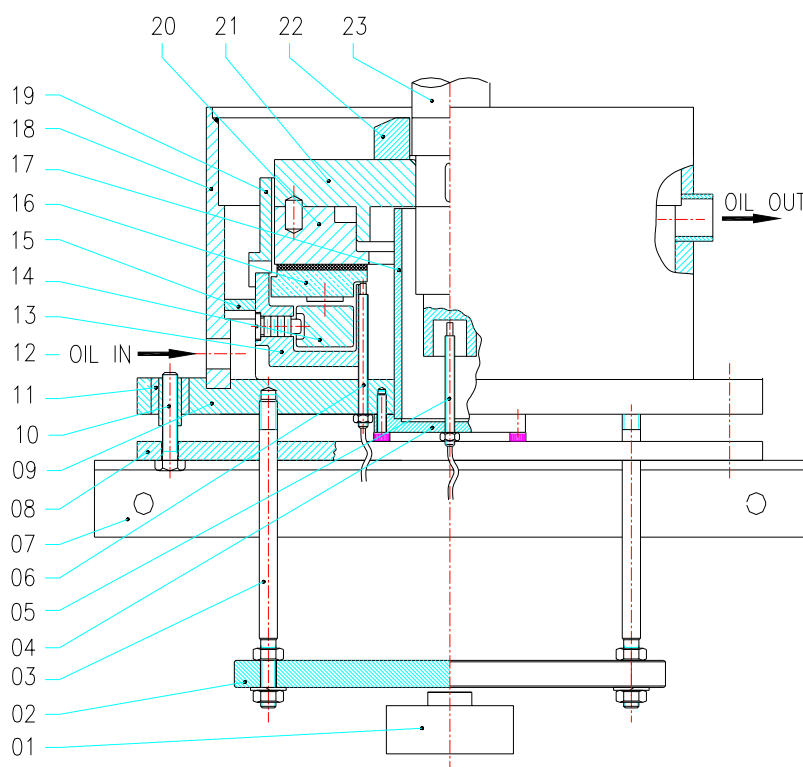
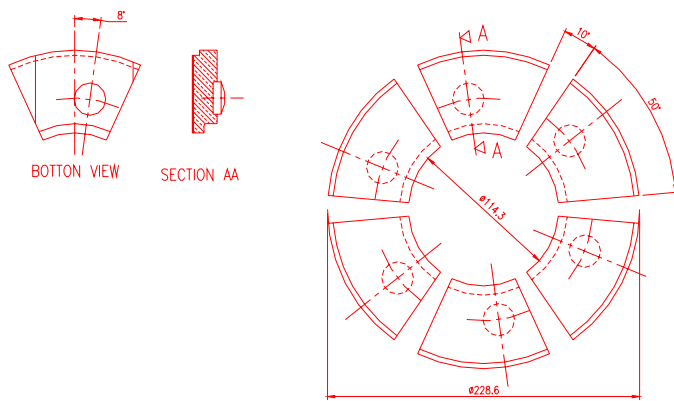


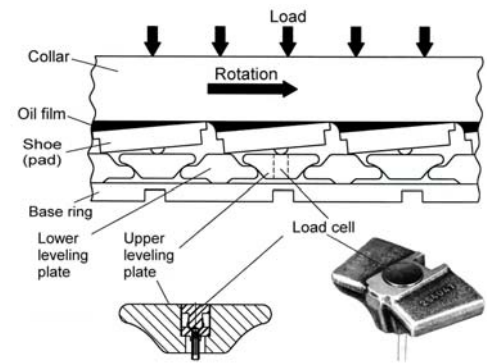
Figure 2. The thrust bearing details showing the proximity sensors, lubricant circulation and loading system.

4. The Test Bearing

Figure 3(a) shows the main dimensions of the test bearing, which is consisted by six sector shaped pads, each of them having a spherical pivot located at 66% of the pad angle, which is equal to 50°. The bearing inner and outer diameters are equal to 114.3 mm and 228.6 mm, respectively. The whole nominal thickness of the pads, measured at the pivot position is equal to 28.58 mm. Each pad is positioned with the pivot on top of the corresponding upper leveling plate, as shown in Fig. 3(b). For the non-rotating condition, the collar remains in contact with the whole flat surface of the pads, without any oil film in the contact surface. Therefore, this situation will be considered as the reference for the proximity sensors installed under one pad. For the collar rotating condition, each pad takes the inclined position and an oil film is established as shown schematically in the Fig.3(b). The thickness of the oil film at the vertical line passing through the pivot point will be denoted by h_p , and it corresponds to the actual lifting of the rotating collar, relative to the reference position of the proximity sensor (05), shown in Fig. 2. Similarly, the oil film thicknesses at the leading (or inlet) and trailing (or outlet) edges of the pad will be denoted by h_i and h_o , respectively.



(a) test bearing main dimensions



(b) working principle of the tilting pad thrust bearing

Figure 3. The test bearing dimensions and shape of the oil film established between the rotating collar and the pads

5. Results and Discussion

The presentation and discussion of the temperature distribution within a pad is made on the basis of Fig.4 and Tab.1. Figure 4 shows the thermocouple positions under the pad babbitted surface and also in the axial direction, through the positions 1, 2 and 6. A photograph of the pivoted pad, prepared for the thermocouple insertions, is also shown.

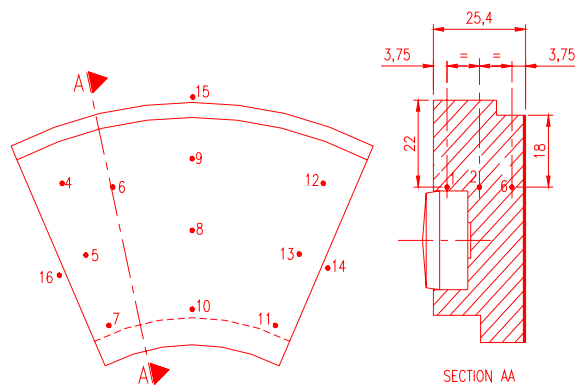


Figure 4. Undersurface and axial thermocouple positions in the pad

Table 1 shows the steady state temperatures, according to Fig. 4, for a 20 kN thrust load, 14 l/min oil flow rate, for rotational speeds of 2000 rpm, 2500 rpm and 3000 rpm, the oil inlet temperature being maintained at about 40°C.

Table 1. Temperature distribution within the pad, for rotational speeds of 2000 rpm, 2500 rpm and 3000 rpm.

Oil Flow Rate: 14 (l/min) Lubricating Oil ISO VG32 Rotational speed: 2000 2500 3000 (rpm)											
Axial Load: 20 (kN)				Pivot Position: 66%				Friction Torque: 11.3 12.3 12.6 (N.m)			
Temperatures °C											
Pos.	Rotational speed (rpm)			Pos.	Rotational speed (rpm)			Pos.	Rotational speed (rpm)		
	2000	2500	3000		2000	2500	3000		2000	2500	3000
T1	51.0	53.6	57.8	T2	52.0	55.0	59.2	T6	56.0	59.6	64.0
T4	55.2	59.1	63.0	T5	56.0	59.6	64.1	T7	54.4	57.5	61.7
T8	52.0	55.3	59.4	T9	50.8	54.1	58.6	T10	50.9	53.9	58.0
T11	46.5	49.5	53.1	T12	46.8	50.7	54.8	T13	48.5	52.0	55.6
T _o	47.7	51.2	55.1	T _i	39.2	40.8	42.2	T14	48.0	51.8	55.3
T _a	23.0	23.8	24.3	T _{bath}	46.7	50.4	54.1	T15	48.0	51.6	55.3

T_a = ambient air temperature;

T_i = inlet oil temperature;

T_o = outlet oil temperature.

Four additional thermocouples give the ambient temperature, T_a , the oil supply temperature, T_i , the outlet oil temperature, T_o , and the oil bath temperature, T_{bath} , over the ring (15), shown in Fig.2. Steady state friction torques, corresponding to the three rotational speeds, are also given in Tab.1.

It is evident from Tab.1 that the steady state temperatures and friction torques increase with the rotational speeds. It may also be seen from Tab.1 that the temperature T6, corresponding to position 6 of Fig.4, is the maximum undersurface operating temperature, while T11 and T12 are the lowest undersurface temperatures. This is important in conjunction with the experimental conclusion by Glavatskikh (2004), showing that the oil film temperature is about 7% higher than the corresponding pad undersurface temperature. The operating temperature of the oil film has fundamental importance for the oil film thickness analysis, as the operating viscosity of the oil is strongly dependent on temperature. Friction torques given in Tab.1, were obtained without the anti-churning ring (19), Fig.2, as it causes a torque increase of about 10%. The friction torques obtained in the present work were about 60% lower than those presented by Glavatskikh (2001) and by Glavatskikh and DeCamillo (2004), for similar conditions of load, speed and oil flow rate. Although the bearing size is the same, Glavatskikh's bearing tilting pads are pivoted at 60% of the pad angle. Also, the existence of some oil guide rings, plus oil seals and the fully flooded lubrication system in the Glavatskikh's test rig, may be the reasons for the significant difference in bearing friction torque.

The presentation and discussion of the oil film thicknesses results is made on the basis of Figs.5, 6, 7 and 8.

Figure 5(a) shows the oil film thicknesses at the pivot position and also for an angular position at about 42° from the pad leading edge, for a 20 kN thrust load, 2000 rpm and oil flow rates varying from 4 l/min to 16 l/min. Temperatures T6 and T12 are also shown, in order to estimate the operating viscosity of the oil. It is seen that, for the oil flow rates above, the oil film thicknesses remains approximately constant for oil flow rates up to about 10 l/min., and increases for oil flow rates above 10 l/min. **Note:** in fact, the oil film thickness for the angular position at 42° from the leading edge was taken from an average value between the outputs from two proximity sensors located at the inner and outer radii of the pad. These outputs gave indication of the occurrence of a pad inclination in the radial direction, besides the expected inclination in the circumferential direction. However, there is a possibility that the instrumented pad was in a lower position relative to the neighboring ones, due to machining tolerances and / or differential wear at the spherical surface of the pivots and leveling plates.

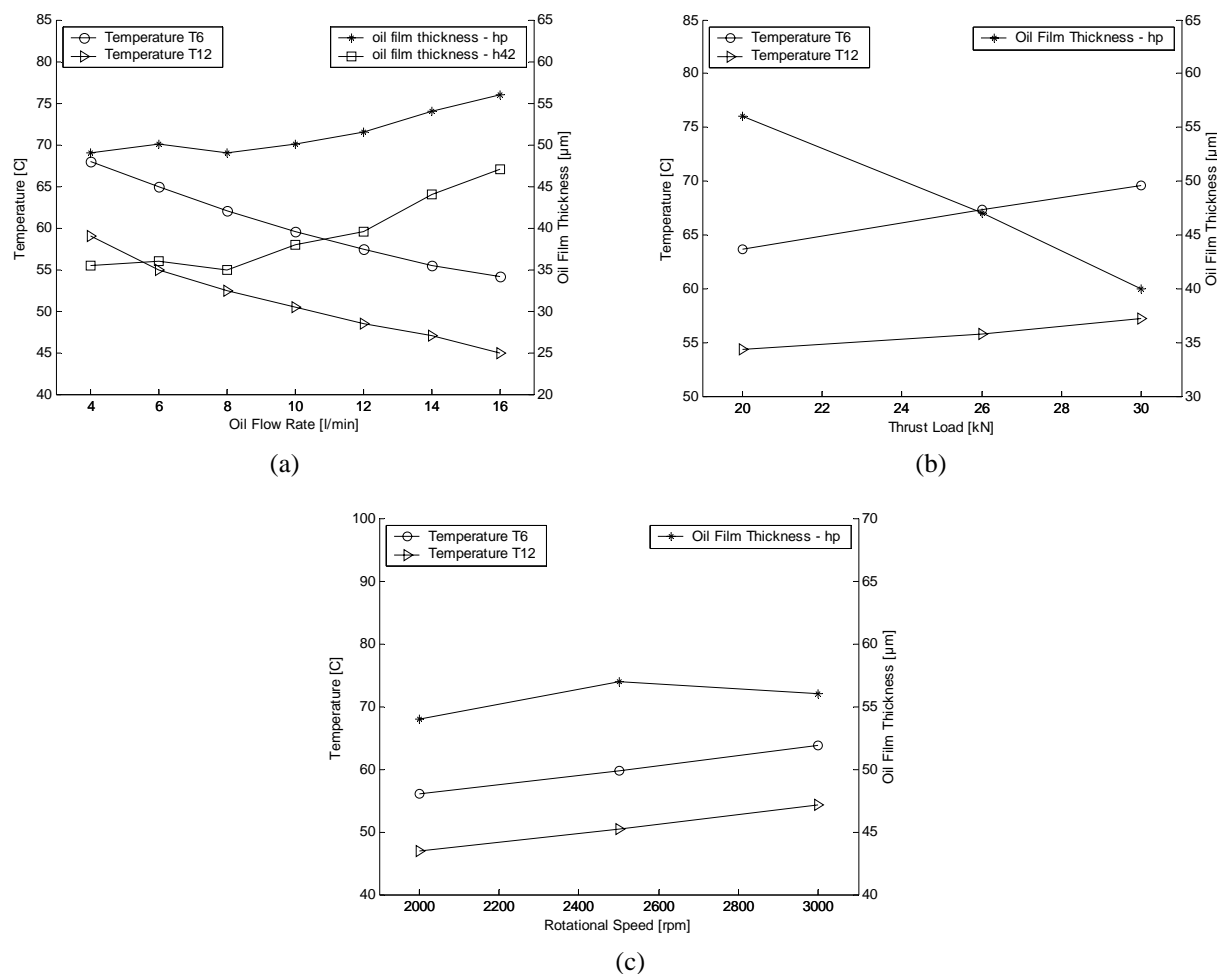


Figure 5. Oil film thicknesses and temperatures versus (a) oil flow rate, (b) thrust load and (c) rotational speeds.

Figure 5(b) shows the variation of the oil film thickness at the pivot position, for a 3000 rpm rotational speed, 14 l/min of oil flow rate and for thrust loads of 20 kN, 26 kN and 30 kN. It is seen that oil film thickness decreases with load, while operating temperatures increase.

Figure 5(c) shows the oil film thickness at the pivot position, for a 20 kN thrust load and 14 l/min oil flow rate, and for rotational speeds of 2000 rpm, 2500 rpm and 3000 rpm. Temperatures T6 and T12 are also shown. It is seen that both the temperatures and the oil film thicknesses increase with rotational speed. However, at 3000 rpm the oil film thickness is lower than the value corresponding to 2500 rpm. This fact will be explained latter, with the help of Fig. 8.

For illustrative purpose, Figs.6, 7 and 8 show the print screen output of the proximity sensor [05] installed near the shaft end, as shown in Fig.2. The vertical scales are given in μm . For reference purpose, Table 2 shows the sensor distance to the shaft end (see Fig.2) obtained from a calibration procedure by varying the thrust load for the machine in the stationary condition.

Table 2. Stationary proximity sensor response versus thrust load applied to the bearing

Thrust load (kN)	20	26	30
Sensor distance (μm)	534	522	518

The captions of the parts (a), (b) and (c) of the Figs.6, 7 and 8, also give the T6 and T12 operating temperatures and the friction torque corresponding to the oil flow rate values. It is important to observe that the variation of the amplitude of the sensor output signal gives a measure of the bearing instability.

Figure 6 shows the oil film thickness behavior for three oil flow rates supplied to the bearing, for a 20 kN thrust load, 2000 rpm and 40°C oil supplied temperature. It can be seen that the oil film thickness increased by about 9 μm when the oil flow rate was increased from 4 l/min. to 16 l/min. Further, from the amplitudes of the proximity sensor outputs corresponding to parts (a), (b) and (c), it is seen that the bearing stability increases as the supplied oil flow rate is increased. This is in agreement with the theoretical data given by Schwarz *et al.*(2003), showing that the higher the rotational speed, the higher the oil flow rate self pumped by the bearing.

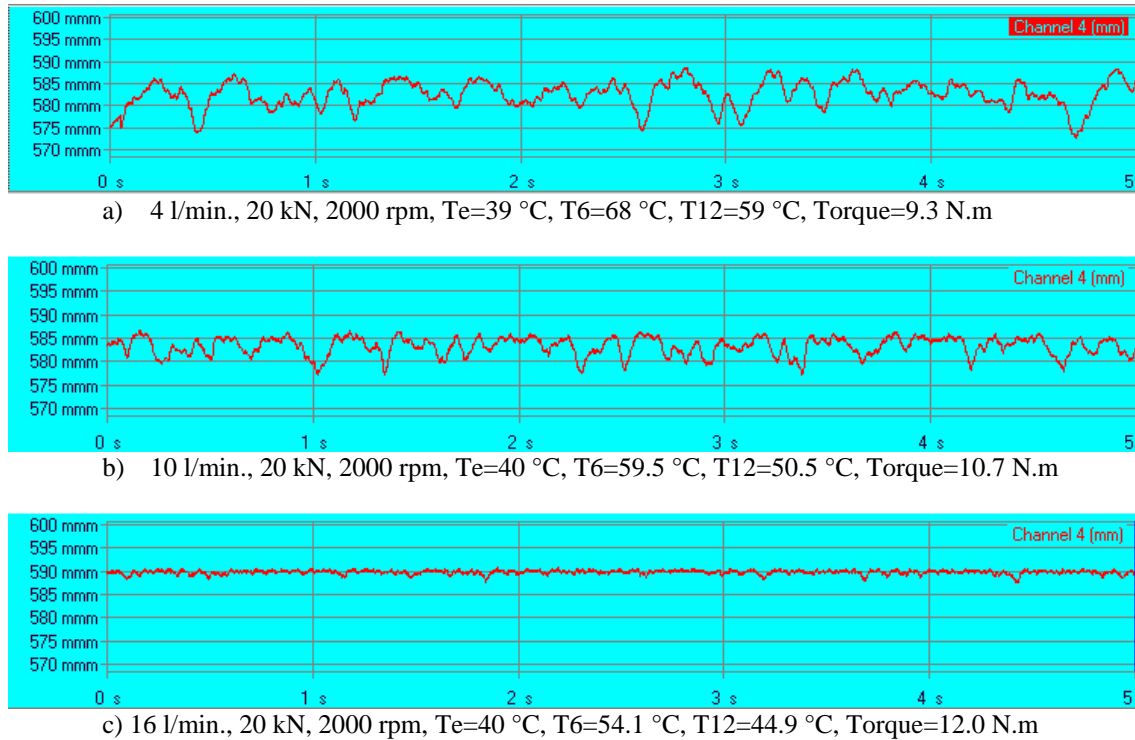
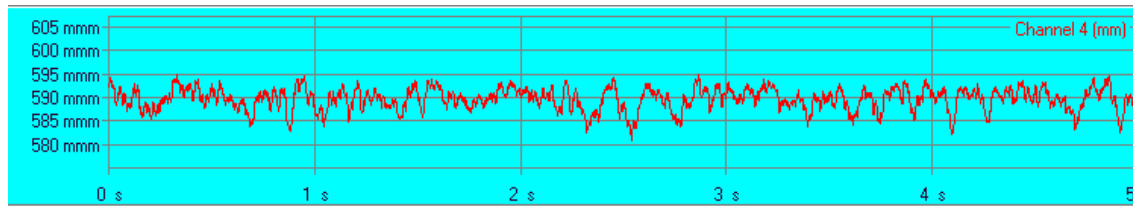
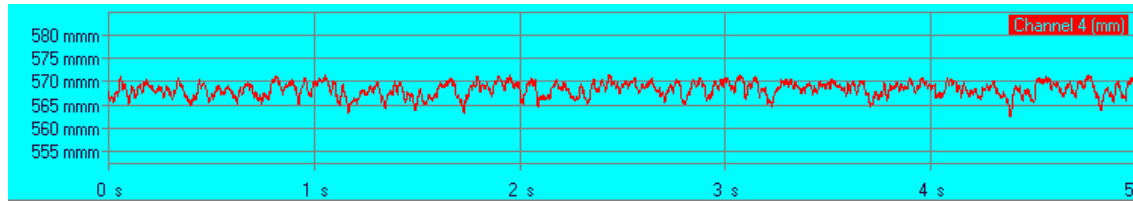


Figure 6. Evolutions of oil film thickness and bearing stability with increasing oil flow rate.

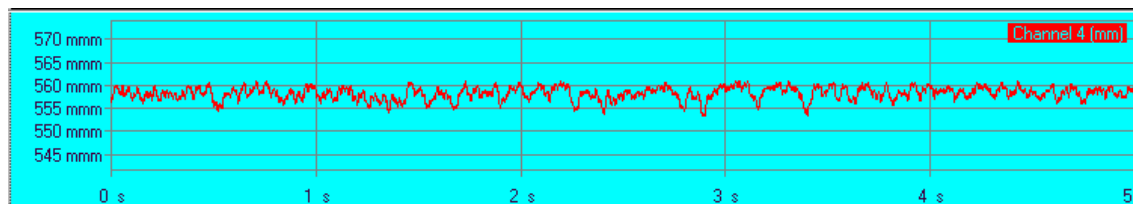
Figure 7 shows how the oil film thickness decreases with thrust load (20 kN, 26 kN and 30 kN) for 3000 rpm rotational speed, 14 l/min. oil flow rate and oil supplied temperature from 40°C to 45°C. It can be seen that the bearing stability increases as the applied load is increased. Also, from the captions of parts (a), (b) and (c) it may be seen that the operating temperatures and friction torque increase with load.



a) 14 l/min., 20 kN, 3000 rpm, $T_e=41.6^\circ\text{C}$, $T_6=63.7^\circ\text{C}$, $T_{12}=54.3^\circ\text{C}$, Torque=12.6 N.m



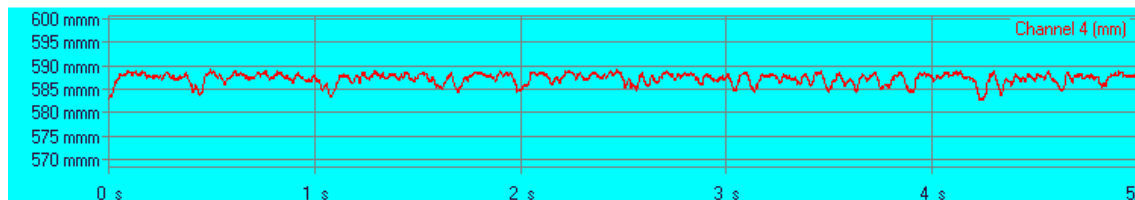
b) 14 l/min., 26 kN, 3000 rpm, $T_e=43^\circ\text{C}$, $T_6=67.3^\circ\text{C}$, $T_{12}=55.8^\circ\text{C}$, Torque=13.9 N.m



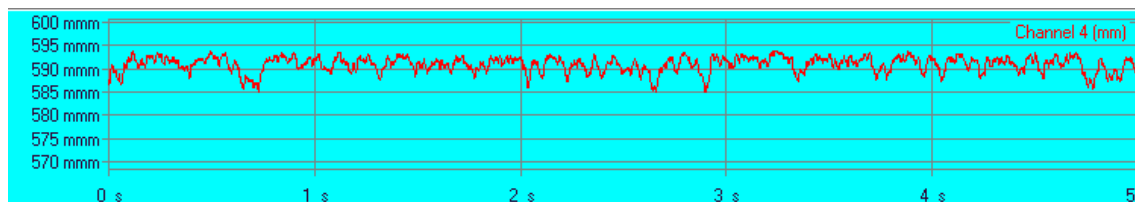
c) 14 l/min., 30 kN, 3000 rpm, $T_e=44.5^\circ\text{C}$, $T_6=69.6^\circ\text{C}$, $T_{12}=57.2^\circ\text{C}$, Torque=14.4 N.m

Figure 7. Variations of oil film thickness, operating temperatures and friction torque with thrust load.

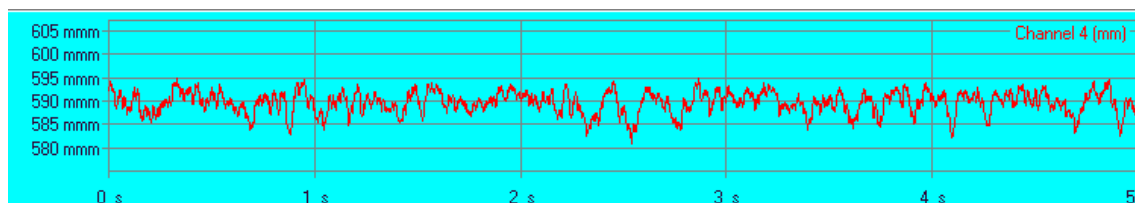
Figure 8. shows how the oil film thickness increases with rotational speed (2000 rpm, 2500 rpm and 3000 rpm) for a 20kN thrust load and 40°C oil supplied temperature. It may also be seen from the amplitudes of the proximity sensor outputs in parts (a), (b) and (c), that the bearing stability decreases with speed, for constant oil flow rate and thrust load.



a) 14 l/min., 20 kN, 2000 rpm, $T_e=40^\circ\text{C}$, $T_6=56^\circ\text{C}$, $T_{12}=47^\circ\text{C}$, Torque=11.3 N.m



b) 14 l/min., 20 kN, 2500 rpm, $T_e=40.5^\circ\text{C}$, $T_6=59.7^\circ\text{C}$, $T_{12}=50.5^\circ\text{C}$, Torque=12.3 N.m



c) 14 l/min., 20 kN, 3000 rpm, $T_e=41.6^\circ\text{C}$, $T_6=63.7^\circ\text{C}$, $T_{12}=54.3^\circ\text{C}$, Torque=12.6 N.m

Figure 8. Evolutions of oil film thickness, operating temperatures and friction torque with increasing rotational speed.

In fact, as can be seen in Fig. 8, oil film thickness was lower at 3000 rpm, than at 2500 rpm. It is also seen, from the torque data on the captions of the figure, that the rate of torque increase at this higher speed range was lower than the rate of torque increase for speeds lower than 2500 rpm. However, for higher oil flow rates supplied to the bearing, both oil film thickness and friction torque would have a more continuous rate of increase.

6. Conclusions

A series of experimental tests has been carried out on a vertical shaft tilting pad thrust bearing, in order to determine the influence of oil the flow rate, the shaft speed, the thrust load and the temperature of the oil supplied to the bearing on the steady state operating characteristics, such as, oil film thicknesses, temperatures and friction torque. The most important conclusions are the following: a) from the oil film thicknesses measurements, it was found that a radial inclination of the pads also takes place, b) the oil film thicknesses and the friction torque increase with oil flow rate, while operating temperatures decrease, c) the oil film thicknesses decrease with thrust load, while temperatures and friction torque increase, the three operating parameters increased with rotational speed, for a given condition of thrust load and oil flow rate. However, there exists a limiting speed above which the oil film thicknesses decrease. Then, by increasing the oil flow rate, oil film thicknesses and oil film stabilization increase again.

7. Acknowledgements

The authors gratefully acknowledge the financial support from FAPEMIG – Fundação de Amparo à Pesquisa do Estado de Minas Gerais, Proc. TEC 855/97, TEC 2280/98 and CNPq 460585/2002-2, plus the technical and financial support from Kingsbury Inc. Further, thanks are due to CAPES from a scholarship.

8. References

- Dadouche, A. Fillon, M. and Bligoud, J.C., 2000, "Experiments on Thermal Effects in a Hydrodynamic Thrust Bearing", *Tribology International*, Vol. 33, pp. 167-174.
- Glavatskikh, S.B., 2001, "Steady State Performance Characteristics of a Tilting Pad Thrust Bearing", *Trans. ASME, Journal of Tribology*, Vol. 123, pp. 608-615.
- Glavatskikh, S.B., 2004, "A Method of Temperature Monitoring in Fluid Film Bearings", *Tribology International*, Vol. 37, pp. 143-148.
- Glavatskikh, S.B. and DeCamillo, S., 2004, "Influence of Oil Viscosity Grade on Thrust Pad Bearing Operation", *Journal of Engineering Tribology, Proc. Instn. Mech. Engrs.*, Vol. 218, Part J, pp. 401-412.
- Gregory, R.S., 1974, "Performance of Thrust Bearings at High Operating Speeds", *J. Lubr. Technol.*, Vol. 96, No. 1, pp. 7-14.
- Schwarz, V.A., Silva, P.F., Vicente, W.M., Dias, J.C. and Kuhn, M.J., 2003, "Effects of the Pivot Position and Lubricant Flow Rate on the Behavior of Sector Shaped Tilting Pads Hydrodynamic Thrust Bearings", *17th International Congress of Mechanical Engineering*, S. Paulo, Brazil, pp. 1-10.
- Yuan, J.H., Medley, J.B. and Ferguson, J.H., 1999, "Spring-Supported Thrust Bearings Used in Hydroelectric Generators: Laboratory Research Facility", *Tribology Trans.*, Vol. 42, No. 1, pp. 126-135.

9. Responsibility notice

The authors are the only responsible for the printed material included in this paper.